Department of Physics and Astronomy
University of Heidelberg

Bachelor Thesis in Physics
submitted by

Yannick Kirchhoff

born in Bonn (Germany)

2018

Study of the influence of modified (non-)strange baryon and meson spectra on hadron densities calculated within the statistical hadronization model

This Bachelor Thesis has been carried out by Yannick Kirchhoff at the
Physikalisches Institut in Heidelberg
under the supervision of
Prof. Dr. Johanna Stachel

Abstract

The statistical hadronization model describes the yields of hadrons produced in heavy-ion collisions.
It successfully calculates and predicts particle yields in a wide range of collision energies. However, thermal fits to LHC data showed a deviation of the proton yields of nearly 3σ. These deviations are known as the proton anomaly.
An earlier study showed that the inclusion of non-strange baryon states in the model enlarged the deviations for the proton yields significantly. It was suggested that this could be due to an imbalance in the implemented hadron spectra.
The influence of the implementation of a more complete set of hadrons into the statistical model is studied in this work. It is shown that the further extension does not reduce the deviations coming from the insertion of non-strange baryon states significantly.
Finally, a correction that makes use of the S-matrix formalism and has which been able to improve the proton anomaly, has been applied to the calculations with the modified spectrum. It turns out that this correction is not able to explain the large deviations and an alternative explanation is presented.

Zusammenfassung

Das Modell der statistischen Hadronisierung beschreibt die in Schwerionenkollisionen entstehenden Teilchenanzahlen.
Es hat sich bei der Berechnung und Vorhersage von Teilchenanzahlen über einen weiten Energiebereich als sehr erfolgreich erwiesen.
Beim Fit der berechneten Teilchendichten an Messungen am LHC ergab sich jedoch eine Abweichung der erzeugten Protonen von fast 3σ. Diese Abweichungen werden als Protonenanomalie bezeichnet.
Eine frühere Arbeit hat gezeigt, dass durch das Hinzufügen von non-strange Baryonen in das Modell die Abweichungen der Anzahl erzeugter Protonen deutlich zunimmt. Es wurde vorgeschlagen, dass diese Verschlechterung des Fits durch ein Ungleichgewicht in den hinzugefügten Hadronen bedingt sein könnte.
In dieser Arbeit wird der Einfluss der Erweiterung des statistische Modells um eine vollständigere Hadronenliste untersucht. Es wird gezeigt, dass diese Erweiterung die Abweichungen durch die zusätzlichen non-strange Baryonen nicht signifikant reduzieren kann.
Schließlich wird eine Korrektur, die auf dem S-Matrix Formalismus beruht und die Protonenanomalie verbessern konnte, auf die Berechnungen mit dem modifiziertem Hadronspektrum angewandt. Es zeigt sich, dass diese Korrektur nicht die großen Abweichungen erklären kann und eine alternative Erklärung wird präsentiert.

Contents

1 Introduction

The Large Hadron Collider (LHC) is the world's most powerful particle accelerator located at the European Organization for Nuclear Research (CERN). The collider has four crossing points with the four main detectors ATLAS[1], CMS[2], LHCb[3] and ALICE[4].
The LHC can accelerate either protons or heavy nuclei (mainly lead). In proton-proton (p-p) collisions it reaches collision-energies of up to 13 TeV, in lead-lead collisions a maximum of $\sqrt{s_{NN}} = 5.02$ TeV is achieved.
The aim of the LHC is to produce and investigate (elementary) particles and new states of matter to check for predictions of physical theories, mainly the standard model of particle physics and physics beyond the standard model, e.g. supersymmetric theories. In 2012 CMS and ATLAS were able to prove the existence of the Higgs-boson in p-p collisions at 7 and 8 TeV [1, 2], a part of the Higgs-mechanism explaining the masses of the $W^{\pm}$- and Z-bosons and of quarks and leptons via the interaction with the Higgs-Field [3, 4].

The main purpose of heavy-ion collisions is to study properties of quantum chromodynamics (QCD).
QCD is the quantum field theory describing the strong interaction between quarks and gluons. The strong interaction is one of the fundamental forces described by the Standard Model of particle physics. The others are the electromagnetic and the weak interaction, gravitation is not described by the Standard Model.
In QCD there are two fundamental concepts, confinement [5] and asymptotic freedom [6]. Confinement describes the phenomenon that quarks and gluons (particles carrying a color charge) are always bound together in hadrons like baryons (three quarks) and mesons (one quark, one antiquark). These hadrons always appear "colorless", meaning there are no free color charges, as there exist free electric charges in QED. This is often explained by the strong coupling of the strong interaction that makes it favorable to create a pair of quark and antiquark as two quarks are separated, producing new hadrons. Confinement prevents the observation of free quarks and gluons, but always only the bound hadron states.
On the other hand, the coupling constant α_s of the strong interaction decreases with increasing energies or decreasing distances, and the quarks behave as asymptotically free particles. The decreasing coupling constant allows for the successful application of perturbative approaches in the regime of high energies and short distances.

[1] **A** **T**oroidal **L**HC **A**pparatu**S**
[2] **C**ompact-**M**uon-**S**olenoid
[3] **L**arge **H**adron **C**ollider **b**eauty
[4] **A** **L**arge **I**on **C**ollider **E**xperiment

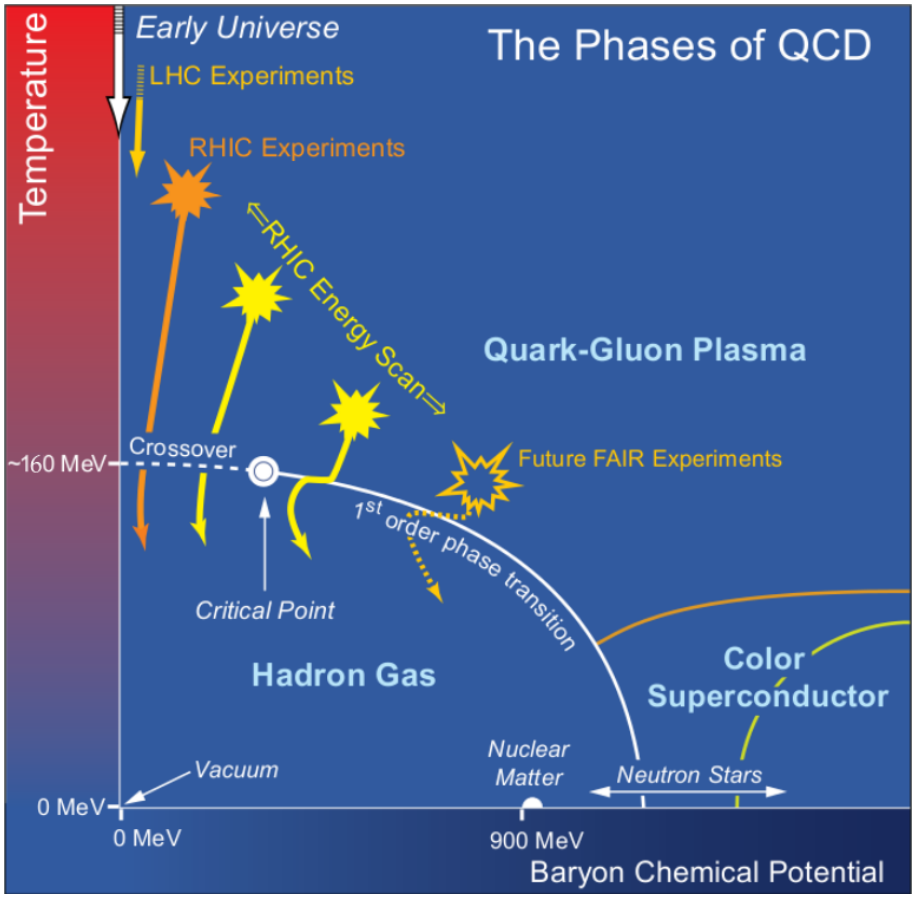

Figure 1: Sketch of the QCD phase diagram. The critical point as well as the region of LHC and RHIC experiments, and the early universe are indicated. Figure taken from [7]

QCD calculations predict a phase diagram in the space of baryochemical potential μ_b and temperature T, as shown in figure 1. For high temperatures or baryochemical potential a phase transition from hadronic matter to a state called Quark Gluon Plasma (QGP) is expected.
This phase transition from hadronic matter to the QGP is expected to be first order for relatively large μ_b and a smooth crossover for nearly vanishing μ_b with a critical point in between. This critical point is a topic of interest, both in theoretical and experimental physics [8, 9].
The QGP is characterized by deconfinement of the quarks and gluons, i.e. they are no longer bound in hadrons, but move freely. Another aspect of the phase transition is a restoration of the chiral symmetry in the QGP phase, meaning a reduction of the quark masses from their constituent mass to their current mass [7]. For the light up- and down-quarks this difference is expected to be by a factor of about 100.
For high μ_b and low temperatures a phase called Color-Flavor Locking (CFL, also Color Superconductor) is expected. In this phase quarks form Cooper pairs, which couple their color properties to their flavor properties.

Heavy-ion collisions are an experimental approach to study the predicted phase diagram. After the collision a fireball of very high energy density is formed. If the energy density is above a critical value (~ 0.3 GeV/fm^3 [10]), it is expected that a QGP is formed. Observations of heavy-ion collisions indicate that a QGP is formed for sufficiently high beam energies [11].
Due to the high pressure through scattering processes the fireball expands and cools down. At a certain critical temperature T_c, the system undergoes a phase transition back to hadronic matter (under the assumption that a QGP was formed before).
In the hadronic phase around T_c, interactions are dominated by inelastic scattering processes. It is assumed that a chemical equilibrium is established even for multi-strange particles through multi-particle scattering, existent at such high particle densities [12].
The system expands and cools down further until the chemical freeze-out temperature T_{ch} is reached. At this temperature, inelastic scattering processes stop and hadron abundances are supposed to be fixed - apart from further decays of unstable particles. As argued in [12], the difference between T_c and T_{ch} can only be of the order of a few MeV, because of the strong dependence of the particle densities on the temperature and the scattering rates on the densities.
It is not clear, if elastic processes continue after the chemical freeze-out until a kinetic freeze-out or if there is just a single - chemical and kinetic - freeze-out [13].
The little difference between T_{ch} and T_c indicates that it is possible to map the phase diagram of QCD quite accurately by measuring the chemical freeze-out temperature at different baryochemical potentials, i.e. different beam energies.

2 The statistical hadronization model

2.1 Statistical mechanics

The statistical hadronization model (SHM) is an approach to describe heavy-ion collisions in the language of statistical physics.
To describe a system with many particles, it is usually inconvenient and unnecessary to solve the differential equation for every particle (microstate). Instead we are only interested in the macrostate described by a few macroscopic parameters, like e.g. temperature or pressure.
These ensemble values are however only well defined if the system is in equilibrium, i.e. the ensemble does not change over time. In statistical mechanics it is principally distinguished between three different ensembles, the microcanonical, the canonical and the grandcanonical ensemble. The properties of all these ensembles are calculated by extremizing the entropy of the system considering the different constraints.
The microcanonical ensemble describes systems with no exchange with their environment. Such a system is therefore characterized by exactly known energy E, volume V and particle number N.
The second important ensemble is the canonical ensemble, which allows for the exchange of energy with its environment. In this kind of system one only knows about the average energy. This constraint leads to a Lagrange multiplier β, given as $\beta = \frac{1}{k_B T}$, when extremizing the entropy. The system is now fully described by the parameters T, V and N.
Finally, the grandcanonical ensemble allows for exchange of energy and particles with the environment. The information about an exact value for the particle number is replaced by the average particle number. In order to fulfill this constraint under the extremization of entropy, another Lagrange multiplier is introduced. This turns out to be $\beta\mu$, where μ is the chemical potential, the energy needed to add a particle to the system.
In the statistical hadronization model, heavy-ion collisions are described by a grandcanonical ensemble. This description requires thermal and chemical equilibrium at the chemical freeze-out. It is assumed that these equilibria are formed in the fireball, due to the high densities and associated short free path lengths. This makes it possible to describe the system as an ensemble.
To obtain thermodynamic properties of an ensemble, it is very useful to calculate the partition function first. The important thermodynamic properties are then given by derivatives of the logarithm (see equations (2.5)-(2.8)).

The partition function for the grandcanonical ensemble is given by [14].

$$\begin{aligned}\mathcal{Z}(T,V,\mu) &= \sum_{N=0}^{\infty} \sum_{\{n_u\}'} e^{-\beta(E(\{n_u\}')-\mu N)} \\ &= \sum_{\{n_u\}} e^{-\beta\sum_u (E(u)-\mu)n_u} = \prod_u \sum_{n_u} e^{-\beta(E(u)-\mu)n_u} \\ &= \begin{cases} \prod_u \frac{1}{1-e^{-\beta(E(u)-\mu)}} & \text{for bosons} \\ \prod_u \left(1+e^{-\beta(E(u)-\mu)}\right) & \text{for fermions} \end{cases}\end{aligned} \tag{2.1}$$

Here n_u is the occupation number of state $u = (\mathbf{p}, m_z)$ with the momentum $\mathbf{p}$ and m_z the z-component of the spin ($n_u = 0, 1$ for fermions and $n_u = 0, 1, 2, ...$ for bosons). $\{n_u\}$' is a combination of occupation numbers which sum up to N and $\{n_u\}$ an arbitrary combination of occupation numbers.
In a relativistic system, like in heavy-ion collisions, the average total particle number is not conserved and has to be replaced by conserved quantities like the average baryon number or strangeness. For a particle i with baryon number B_i, third component of isospin I_{3_i}, strangeness S_i and charm C_i, we therefore get:

$$\mu_i = \mu_B B_i + \mu_{I_3} I_{3_i} + \mu_S S_i + \mu_C C_i \tag{2.2}$$

With the partition function one can construct the grandcanonical potential (in the following upper signs label bosons, lower signs fermions)

$$\Phi(T,V,\mu) = -\beta^{-1}\log\mathcal{Z} = \pm\beta^{-1}\sum_u \log\left(1 \mp e^{-\beta(E(u)-\mu()}\right) \tag{2.3}$$

The sum can be split up in one sum over $\mathbf{p}$ and one over m_z and we use that $E(u) = E(\mathbf{p}) = \sqrt{p^2c^2 + m^2c^4}$. By taking the limit of infinite volume we get:

$$\begin{aligned}\Phi_i(T,V,\mu) &= \lim_{V\to\infty} \pm\beta^{-1}\sum_{m_z}\sum_{\mathbf{p}} \log\left(1 \mp e^{-\beta(E_i(\mathbf{p})-\mu_i)}\right) \\ &= \lim_{V\to\infty} \pm g_i\,\beta^{-1}\frac{1}{\Delta}\sum_{\mathbf{p}} \Delta\,\log\left(1 \mp e^{-\beta(E_i(\mathbf{p})-\mu_i)}\right) \\ &= \pm g_i\,\beta^{-1}\frac{V}{2\pi^2\hbar^3}\int_0^\infty dp\,p^2\,\log\left(1 \mp e^{-\beta(E_i(\mathbf{p})-\mu_i)}\right)\end{aligned} \tag{2.4}$$

Here we used the spin degeneracy factor g_i, the volume of a discrete momentum $\Delta = \left(\frac{2\pi\hbar}{L}\right)^3$ and $\int d^3p = 4\pi\int_0^\infty dp\,p^2$.

To obtain thermodynamic properties from this, the following equations can be used

$$n_i = -\frac{1}{V}\left(\frac{\partial \Phi_i}{\partial \mu_i}\right)_{V,T} \tag{2.5}$$

$$\epsilon_i = \frac{1}{V}\left(\frac{\partial(\Phi_i\,\beta)}{\partial \beta}\right)_{\beta\cdot\mu_i} \tag{2.6}$$

$$s_i = -\frac{1}{V}\left(\frac{\partial \Phi_i}{\partial T}\right)_{V,\mu_i} \tag{2.7}$$

$$P_i = -\left(\frac{\partial \Phi_i}{\partial V}\right)_{T,\mu_i} = \frac{1}{\beta\,V} log(\mathcal{Z}_i) \tag{2.8}$$

with n_i the particle density, ϵ_i the energy density, s_i the entropy density and P_i the partial pressure.
The quantity of interest in this work is the particle density n_i.
Calculating (2.5) by using equation (2.4) yields:

$$n_i = \frac{g_i}{2\pi^2\hbar^3}\int_0^\infty dp\,\frac{p^2}{e^{\beta(E_i(p)-\mu_i)}\pm 1} \tag{2.9}$$

2.2 Adapting statistical mechanics to heavy-ion collisions

As shown above, heavy-ion collisions can be described as a grandcanonical ensemble with six parameters in general: T, V, μ_b, μ_{I_3}, μ_S and μ_C.
V, μ_{I_3}, μ_S and μ_C can be fixed by conservation of baryon number, third component of isospin, strangeness and charm, respectively:

$$V\sum_i n_i B_i = Z + N \tag{2.10}$$

$$V\sum_i n_i(\mu_{I_3}) I_{3_i} = \frac{Z-N}{2} \tag{2.11}$$

$$\sum_i n_i(\mu_S) S_i = 0 \tag{2.12}$$

$$\sum_i n_i(\mu_C) C_i = 0 \tag{2.13}$$

where Z is the number of protons and N the number of neutrons involved in the collision. Therefore we are left with the two free parameters T and μ_b, and the system parameters Z and N, describing the characteristics of the colliding nuclei.
To take interactions between particles into account, one has to make some corrections to the model:
As shown in [15], attractive interactions between particles can be taken into account by treating resonances as stable particles. However, this is only valid under the assumption of

"sharp resonances", meaning that the resonance can be approximated as a delta function. Repulsive interactions are treated with an eigenvolume correction after Rischke, Gorenstein, Stöcker and Greiner [16] in a similar manner to the van-der-Waals model. Particles are approximated as hard spheres with a radius R, and are prohibited to come closer to each other than 2R ($R = 0.3$ fm for mesons and baryons is used).
In this approach the accessible volume is reduced due to the eigenvolume of the particles, leading to an iterative formula for the chemical potential and the pressure given by:

$$P^{excl}\left(T,\,[\mu_i]\right) = P\left(T,\,[\hat{\mu}_i]\right) \tag{2.14}$$

$$\hat{\mu}_i = \mu_i - v_{0,i}\,P^{excl}\left(T,\,[\mu_j]\right) \tag{2.15}$$

with the eigenvolume $v_{0,i}$ of the particle. Here $[\mu_i]$ means the tuple $\mu_1, ..., \mu_n$.
This leads to a corrected particle density

$$n_i^{excl}\left(T,\,[\mu_j]\right) = \frac{n_i\left(T,\,\hat{\mu}_i\right)}{1 + \sum_j v_{0,j}\,n_j\left(T,\,\hat{\mu}_j\right)} \tag{2.16}$$

The other thermodynamic properties are corrected in a similar way.
The numerical implementation of the statistical hadronization model is realized by the thermal code. It contains all information about the considered hadron species needed for the calculations, like e.g. the mass, the spin degeneracy, isospin and charge. Crucial for the calculation of hadron yields are the information about decays and branching ratios, also listed in the code.
The code fulfills the constraints given by the conservation laws (2.10, 2.11, 2.12, 2.13) by using a loop for every conservation law and one inner loop for the iterative volume correction (2.14, 2.15). In the loops the respective chemical potentials are adjusted until the deviations become negligible.
After the calculation of the primordial densities, relevant decays are taken into account. This is done by constructing a vector $\vec{P}$, with the components P_i containing the primordial hadron densities and a decay matrix $\hat{D}$. The entries D_{ij} of the decay matrix are given by the number of particles of type j, produced in a decay of a particle of type i. The densities after decays are then given by

$$\vec{A} = \sum_{n=0}^{N} \vec{P}^{\,\mathbf{T}}\hat{D}^n \tag{2.17}$$

where N is chosen in a manner that there are no unstable particles left. The components A_j now contain information about the densities of particles, either directly measurable in a detector or reconstructable from measured particle densities.
The calculated hadron yields are fitted to experimental data from heavy-ion collisions with fit parameters T_{ch} and μ_b. The fit routine uses a χ^2-minimization.

2.3 Motivation of this work

The statistical hadronization model has shown great success in describing heavy-ion collisions in a wide range of energies. It is able to reproduce measured hadron yields from energies at SPS[5] [17] and RHIC[6] [18], up to LHC energies [19].
However, the fit to data from the ALICE detector shows a large deviation of proton and antiproton yields of 2.7 and 2.9 sigma, respectively. This is often referred to as a "proton anomaly" [19, 20].
It was thought that this proton anomaly could be due to an incomplete hadron spectrum. This idea was supported by results from lattice QCD predicting numerous unknown low mass baryon states.
In [21] a study of the influence of a modified light flavor hadron spectrum was carried out. The implementation of N^* and Δ resonances from lQCD calculations led to an even worse fit with a significant drop in temperature and a deviation of proton and antiproton yields of considerably more than $3\,\sigma$.
A possible explanation given in that study was that there is an imbalance in the implemented hadrons, because only non-strange baryons were taken into account.
The main objective of this work is to investigate the shown deterioration and the appearing proton anomaly by the further implementation of strange baryons and (non-)strange mesons into the model.

[5] **S**uper **P**roton **S**ynchrotron
[6] **R**elativistic **H**eavy **I**on **C**ollider

3 Modified hadron spectra

The current code contains a total of 555 states, divided into 223 mesonic states (123 non-strange, 32 strange, 40 charmed and 28 bottom mesons) and 332 baronyic states (104 non-strange, 96 strange, 56 charmed and 14 bottom baryons). Besides single baryons, the baryonic states also contain light nuclei and hypernuclei like ${}^{3}_{\Lambda}H$ adding up to a total of 62 states.
As mentioned before the influence of the implementation of theoretical hadron states on produced hadron yields will be investigated in this work. In [21] a study of the influence of non-strange baryons was carried out. The hadron spectrum given there will be extended by strange baryon and (non-)strange meson states.
These bound states, in principle, obey the equations of Quantum chromodynamics (QCD). However, the calculation and analysis of properties of these states leads to some problems. QCD-equations cannot be solved analytically and approaches with perturbation theory fail at these low energies (around the rest mass of nucleons), because the strong coupling constant is close to unity.
There are several different approaches to tackle these problems. Two of these, namely lattice QCD and the relativistic quark model, will be used to obtain the theoretical hadron states.

3.1 Baryon states from lQCD

Lattice quantum chromodynamics (lQCD) is a discretized theory. In this approach the equations of QCD are solved on a discretized four-dimensional spacetime (of finite size). In order to receive physical results, the limit of vanishing lattice spacing is taken.
The problem of lQCD calculations is that the calculations are performed with much higher (nonphysical) quark masses to guarantee for a fast convergence. In [22] a lattice of $16^3 \times 128$ with pion masses of $m_\pi = 391$ MeV was used. The results from this paper are used to obtain the properties of theoretical baryon states.

Figures 2(a), 2(b), 2(c) and 2(d) show the plots of the baryon spectra calculated in [22]. The red lines in the plots indicate the mass limit for used baryon states. It is $m_{max} = 2300\,MeV$ for Λ-baryons, Σ-baryons and Ξ-baryons and $m_{max} = 2500\,MeV$ for Ω-baryons.
To obtain excited baryon states with physical masses, known states were identified in the lQCD calculations by looking at the mass ordering, total angular momentum and parity. From the identified hadrons, a scaling factor f was calculated for every particle type. This scaling factor is the ratio between the mass of the known state and the calculated mass. The calculated scaling factors for the different inserted particles are shown in table 1.

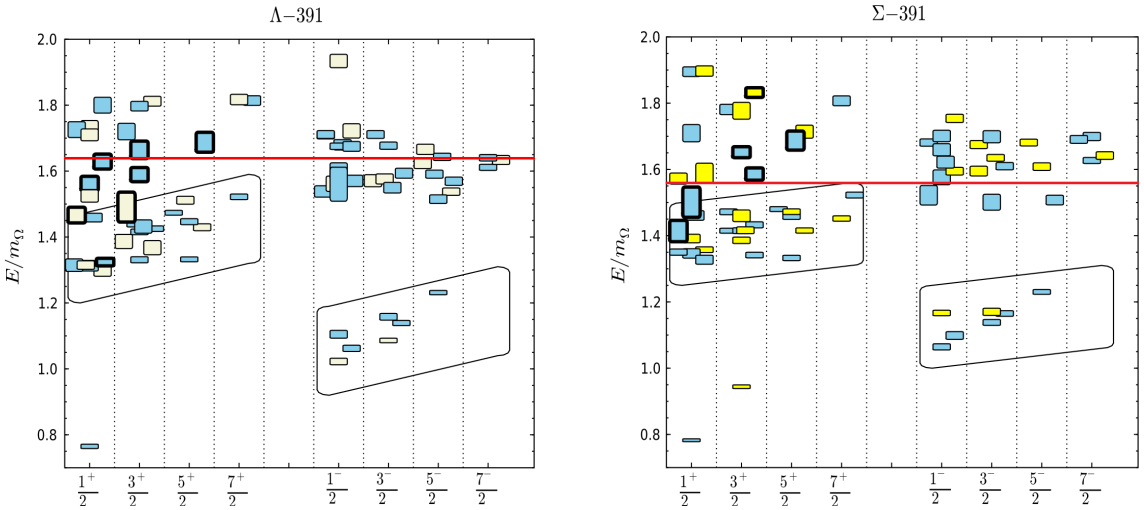

(a) Λ-baryons (b) Σ-baryons

(c) Ξ-baryons (d) Ω-baryons

Figure 2: Excited baryon spectra from lQCD calculations [22]

Partice type	f_{mean}	$\left(\frac{\Delta f}{f}\right)_{max}$	$\left(\frac{\Delta f}{f}\right)_{mean}$
Λ	0.85	0.15	0.054
Σ	0.88	0.15	0.046
Ξ	0.95	0.031	0.024
Ω	1	–	–

Table 1: Calculated scaling factors and maximal deviation

The scaling factor for Ω-baryons is taken as unity, because the masses are given in units of calculated m_Ω. Therefore it is expected to get physical masses for these resonances.

3.2 Meson states from the relativistic quark model

Theoretical meson states are obtained from results of the relativistic quark model given in [23]. This model is a quasipotential approach to calculate the masses of excited states of mesons and baryons consisting of the light u, d and s quarks.
Mesons are described by a wave function of a quark-antiquark state with a fully relativistic treatment of the light quarks. In this description the quark constituent masses $m_u = m_d = 0.33$ GeV and $m_s = 0.5$ GeV are used. For a more detailed description see [23].
The masses of meson states calculated in the framework of the relativistic quark model are in good agreement with known states. Therefore the calculated masses are assumed to be physical masses.
A mass limit of 1700 MeV for non-strange mesons and 1800 MeV was used, leading to a total of 8 non-strange and 16 strange meson states.

3.3 Overview of the different spectra

With the theoretical (non-)strange baryon and meson states several hadron spectra are constructed. Table 2 gives an overview of these spectra.

All three modified spectra are extensions of the original spectrum. Spectrum 1 contains the additional non-strange baryons presented in [21], spectrum 2 contains all theoretical (non-)strange baryon states and spectrum 3 considers all (non-)strange baryon and meson states.

	original	**spectrum 1**	**spectrum 2**	**spectrum 3**
total	555	619	825	849
non-strange mesons	123	123	123	131
strange mesons	32	32	32	48
non-strange baryons	104	168	168	168
strange baryons	96	96	302	302

Table 2: Overview of the constructed hadron spectra. A more detailed overview of the properties of the implemented strange baryons and (non-)strange mesons is given in appendix A and B. For properties of the non-strange baryons see [21]

3.4 Decay properties

The thermal code does not only calculate particle densities due to statistical physics but also takes into account the decays of these particles. Therefore one needs to know about the decay properties of the implemented particles. If there are states with known branching ratios and similar mass and angular momentum, the value of these is taken. Otherwise the branching ratios are approximated by

$$d\Gamma = \frac{1}{32\pi^2}|\mathcal{M}|^2 \frac{|\mathbf{p}_1|^2}{M^2} d\Omega \tag{3.1}$$

for two-body decays with M being the mass of the decaying particle and

$$\mathbf{p}_1 = \mathbf{p}_2 = \frac{[(M^2 - (m_1 + m_2)^2)(M^2 - (m_1 - m_2)^2)]^{\frac{1}{2}}}{2M}$$

the rest frame momentum of the particles, the decay matrix element $\mathcal{M}$ and the solid angle of the particle $d\Omega$ [24].

4 Results

In this section results of the statistical hadronization model with different hadron spectra are presented.
First the development of the ratio between proton- and pion-densities at a fixed temperature of 155.5 MeV is shown.
In the second part, the relative difference of calculated densities for the modified spectra with respect to the unmodified spectrum is examined, again at a temperature of 155.5 MeV.
After that, a fit of the calculated hadron densities to data from the ALICE experiment is caried out and the extracted freeze-out temperatures and the χ^2 of the fits are compared.
Finally a correction of the calculated densities, using the S-matrix formalism, is applied in the fits.
All calculations in this section are performed with a baryochemical potential $\mu_b = 0.7$ MeV, as obtained in the latest fit in [25]. The fits in the last parts are executed with a fixed $\mu_b = 0$ MeV, as the difference is negligible.

4.1 p/π-ratio at $T = 155.5$ MeV

The p/π-ratio, the ratio between calculated densities of protons and pions, can be understood as a measurement of the freeze-out temperature. Therefore it is an interesting and meaningful quantity to study in the context of the statistical hadronization model.
Figure 3 shows the p/π-ratio for the different hadron spectra.

Including the N^*- and Δ-resonances increases the ratio of proton- to pion-yields by a factor of about 1.45. This can be explained by the fact that the implemented resonances produce on average one nucleon and a few pions. Nonetheless the relative change is larger for the protons than for the pions due to the more abundant production of pions.
Implementing additional strange baryons in the model has a similar, but - because of higher masses of implemented states - significantly weaker effect.
The implemented meson states mainly decay into pions and do not produce any protons. As a result, there is a slight reduction of the ratio.
As mentioned above, the development of the p/π-ratio already reveals interesting information, without comparing the calculations to any experimental data.
Figure 4 shows the calculated p/π-ratio as a function of the temperature for the original hadron spectrum. The trend of increasing p/π-ratio with increasing temperature is characteristic for the model and (mostly) independent of the implemented hadron spectrum. A rising temperature leads to an increasing production of heavier resonances. This has a similar effect on the production of pions and protons as the implementation of more resonances into the spectrum.

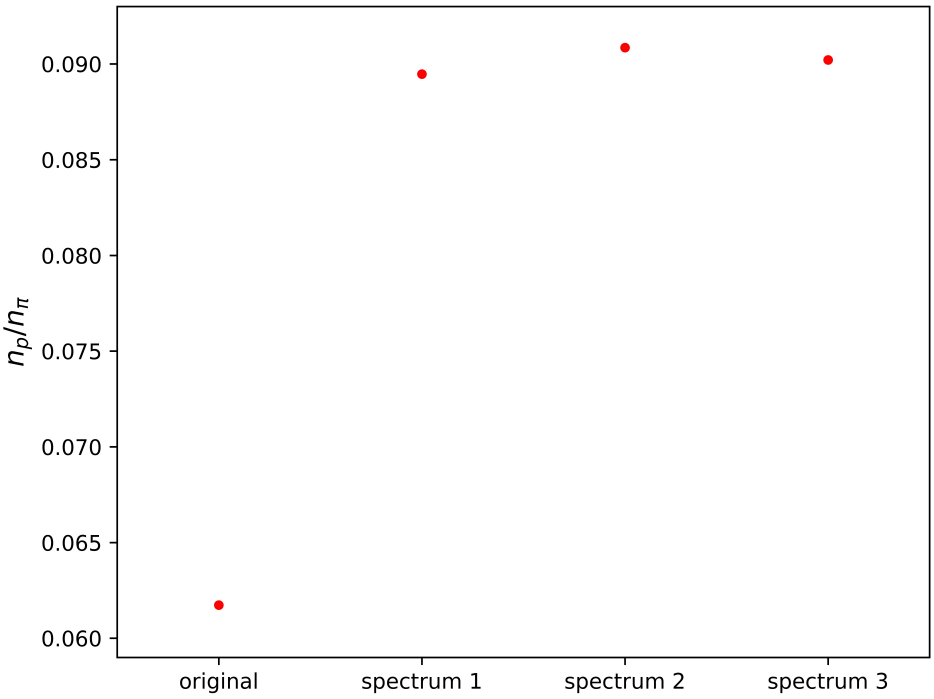

Figure 3: p/π-ratio for the different hadron spectra at $T = 155.5$ MeV

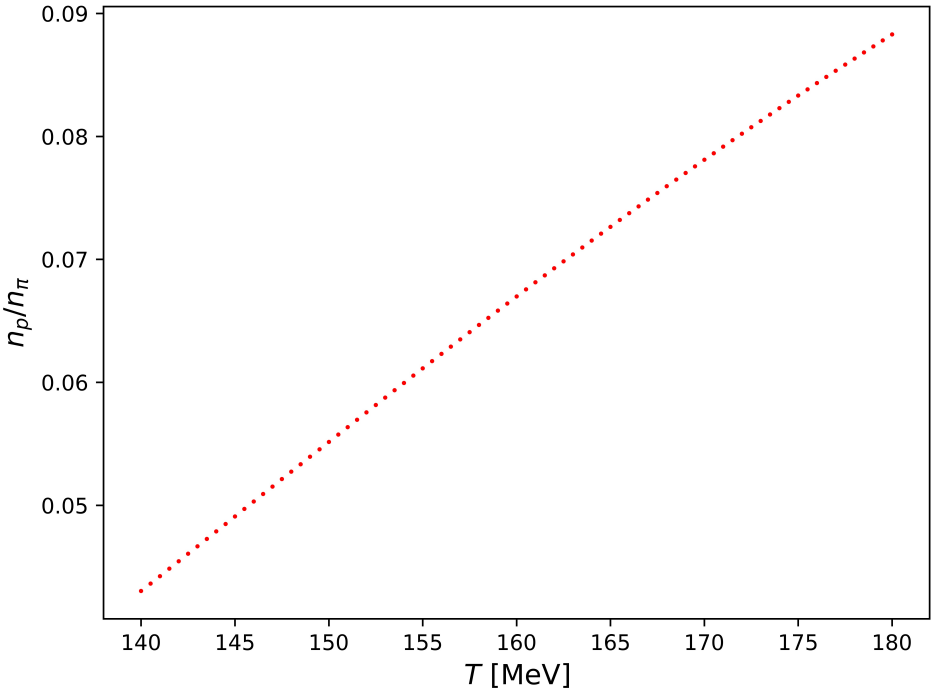

Figure 4: p/π-ratio as a function of the temperature for the original hadron spectrum

This means that - in order to compensate for the higher p/π-ratio from implemented baryon states - we expect a drop in the freeze-out temperature. On the other hand including also meson states is expected to increases the temperature.
This result shows the significance of a balanced hadron spectrum.

4.2 Changes in produced hadron densities

The fit uses a total of 22 particles. Thus it is also important to take a look on how the densities of the other particles change.
Figures 5(a), 5(b) and 5(c) show the density ratios between the three modified spectra and the unmodified one for these 22 particles.
One can clearly see that N^* and Δ resonances mainly affect the densities of (anti-)protons, which increase by 51.6% and have only a little effect on the π- and Λ-densities with 4.6% and 1.2%, respectively. This is due to the decays of the included states. The other densities slightly decrease because of the eigenvolume correction. An increasing number of particle states leads to a larger demoninator in equation (2.16), resulting in a reduced particle density.
The further inclusion of strange baryons mainly gives rise to enlarged Λ-, Ξ- and Ω- densities by 16.1%, 10% and 10.6%, respectively. A slightly increased production of protons (3.4%), pions and kaons (both $\sim 1\%$) can also be observed.
Finally, including meson states in the model, raises the densities of produced pions and kaons by a fraction of a percent.

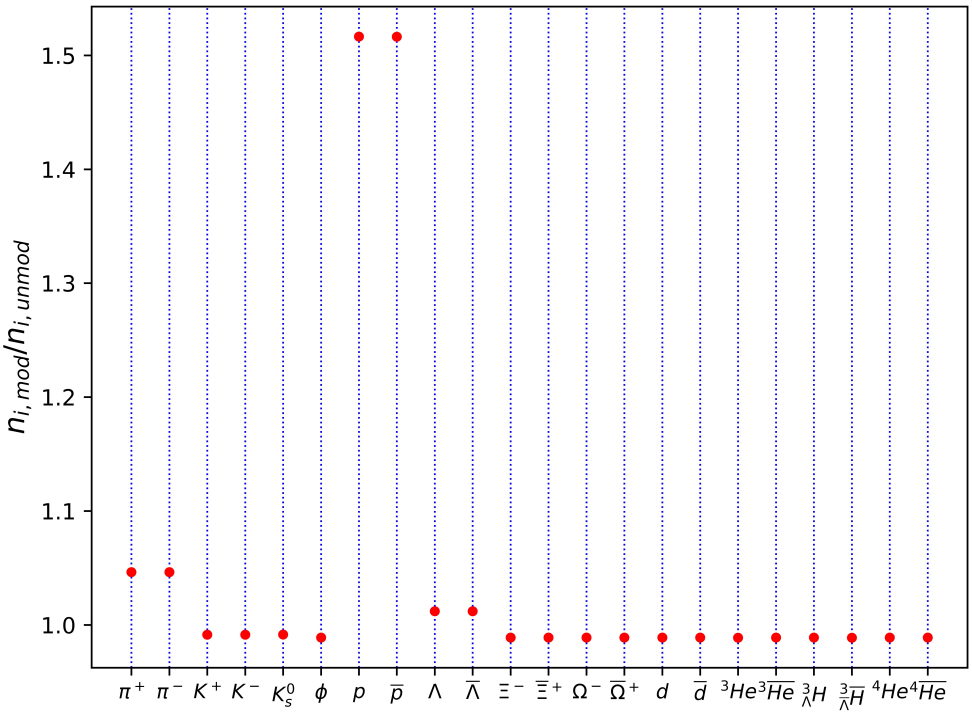

(a) Ratios for the modified hadron spectrum 1

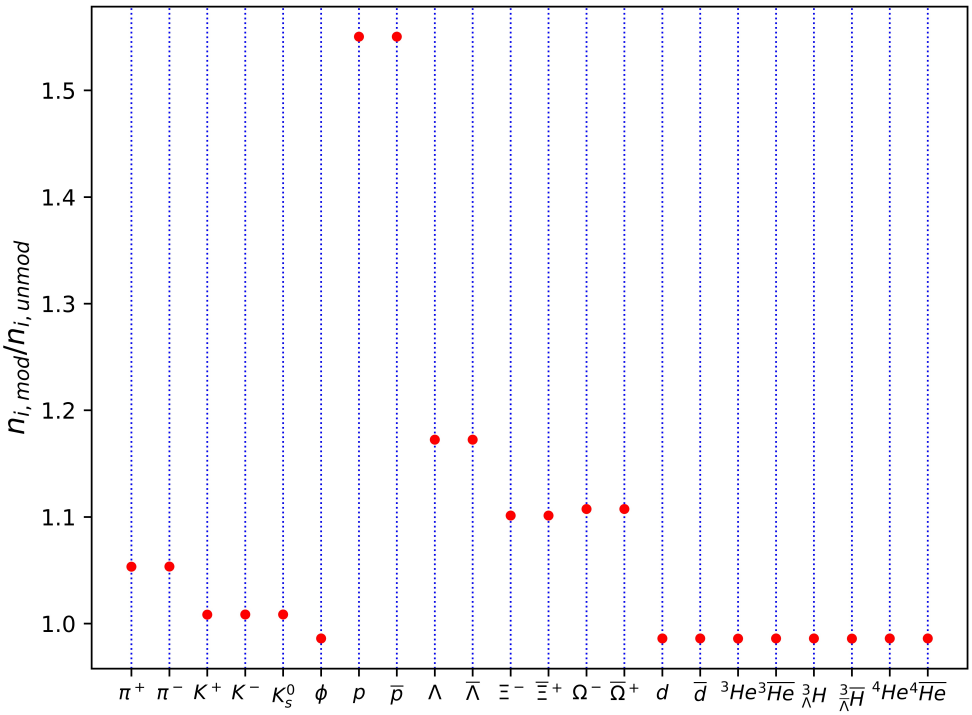

(b) Ratios for the modified hadron spectrum 2

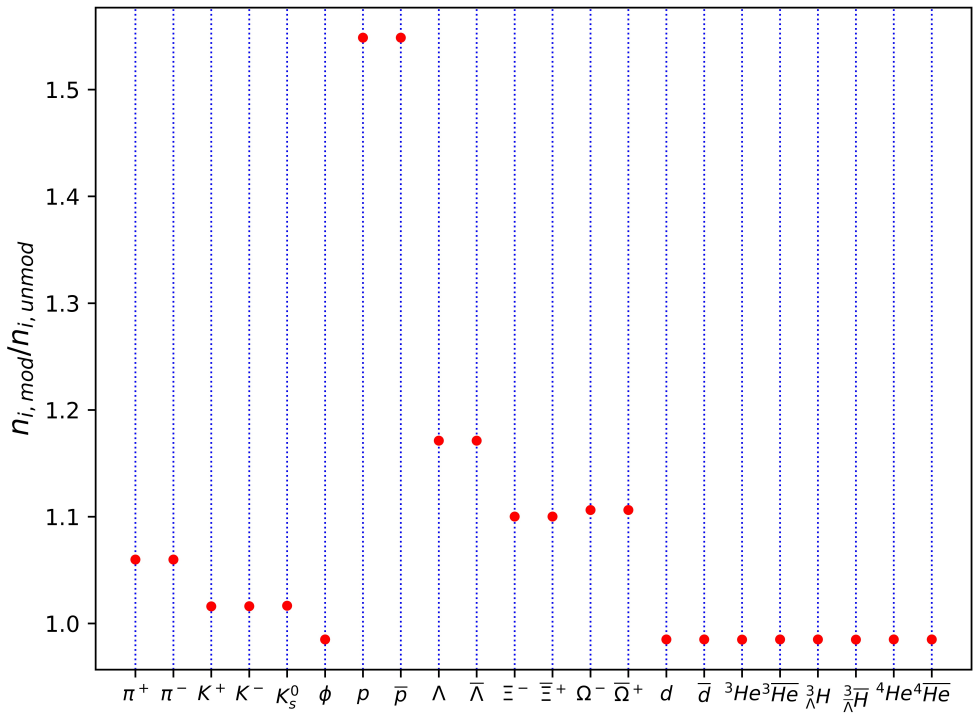

(c) Ratios for the modified hadron spectrum 3

Figure 5: Ratios between densities calculated with and without modified hadron spectra at $T = 155.5$ MeV

4.3 Fit to data from ALICE

After comparing particle densities and ratios calculated with the different hadron spectra, these densities will now be fitted to data from Pb-Pb collisions at ALICE taken in 2012 at $\sqrt{s_{NN}} = 2.76$ TeV with a centrality of 0-10%.

4.3.1 Fit using the original hadron spectrum

At first current results of the statistical hadronization model are presented.
Figures 6 and 7 show the fit to ALICE data and the relative difference between data and fit for the unmodified hadron spectrum, similar to the fits shown in [25].

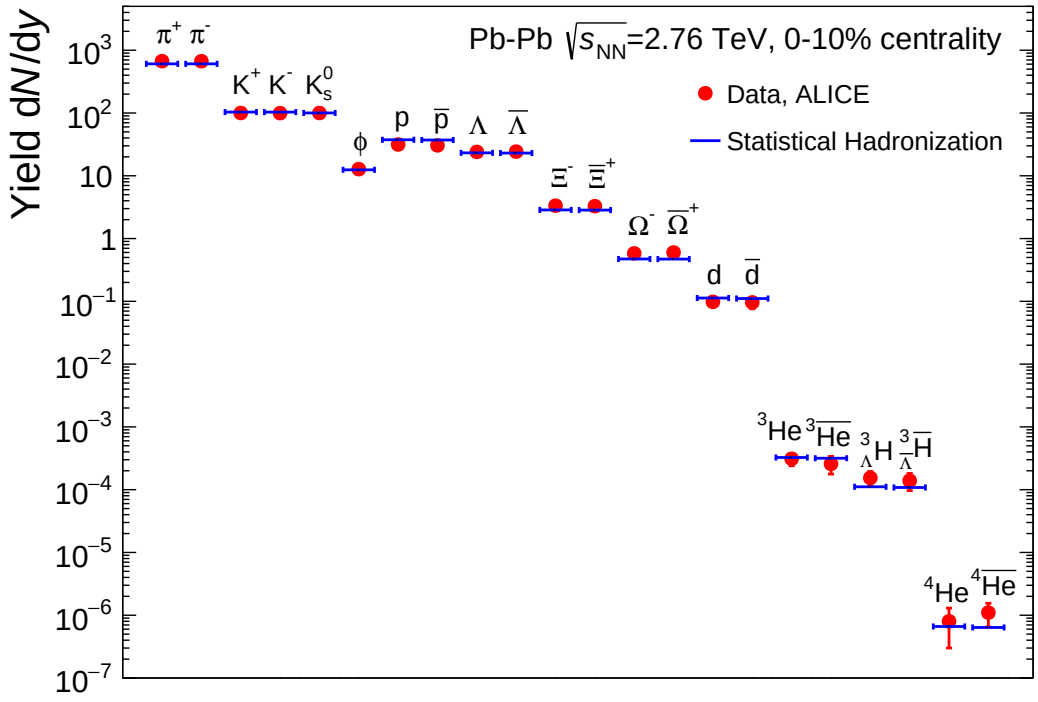

Figure 6: Particle multiplicities measured at ALICE with best fit using the original hadron spectrum

The fit yields a freeze-out temperature of $T_{ch} = 155.5$ MeV and shows a good overall agreement to the data with a reduced $\chi^2/d.o.f.$ of 31.5/20.
However, the yields of the (anti-)protons deviate by slightly below 3σ. These large deviations are the above mentioned "proton anomaly".

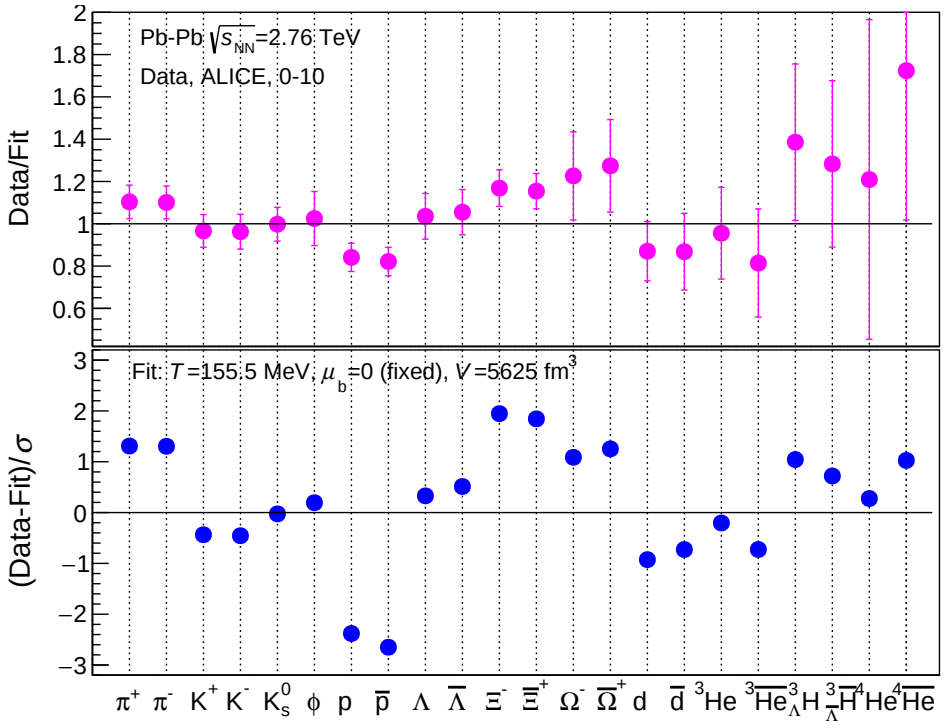

Figure 7: Relative difference between data and best fit using the original hadron spectrum

4.3.2 Fit using the modified hadron spectrum 1

In this section the fits with the N^*- and Δ-states as presented in [21] are presented. As a result of a slightly changed underlying hadron spectrum, the results differ a little to the fits shown in that thesis.

The fit to data and the relative differences between fit and data are shown in figures 8 and 9.
Including non-strange baryon resonances to the hadron spectrum, changes the fit significantly. A drop in the freeze-out temperature to T_{ch} = 151.5 MeV appears, as it was already predicted from the increased p/π ratio. The deviation of the (anti-)proton yields increases to 6.2σ and 6.5σ respectively. This is more than twice as much as before. Furthermore the fit gets worse with an increased $\chi^2/d.o.f.$ of 161/20.

To check if the deterioration of the fit using the modified spectrum 1 is due to an imbalance in the implemented hadrons, as it was suggested in [21], fits of the densities calculated with the hadron spectra 2 and 3 to the same data are carried out. These fits are presented in the following two parts.

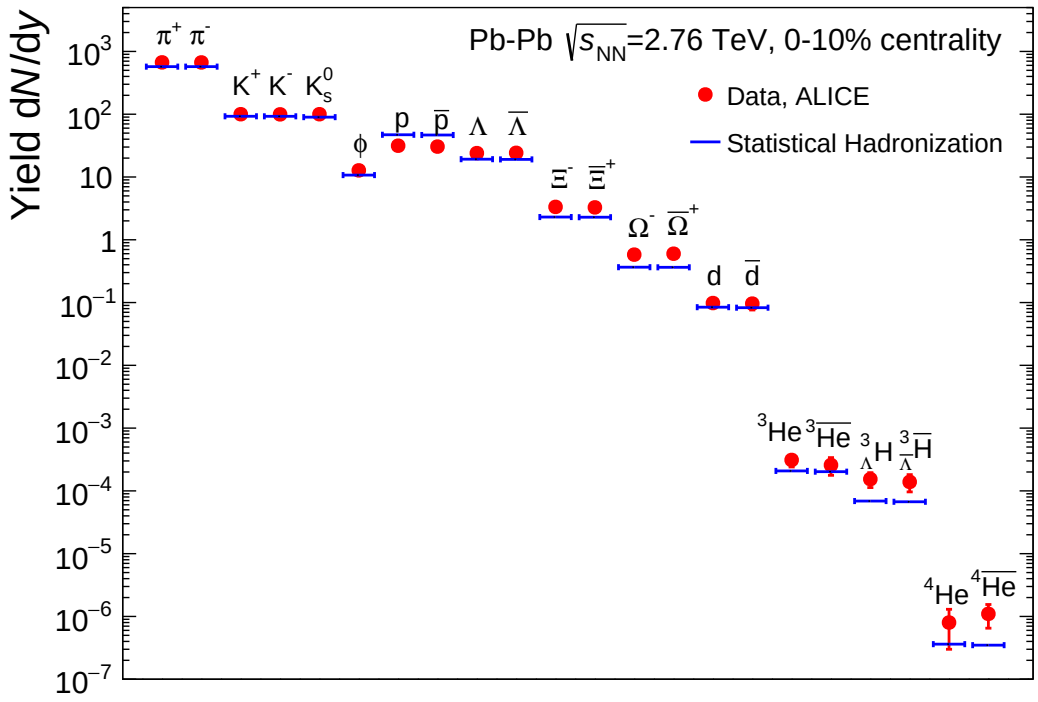

Figure 8: Particle multiplicities measured at ALICE with best fit using the modified hadron spectrum 1

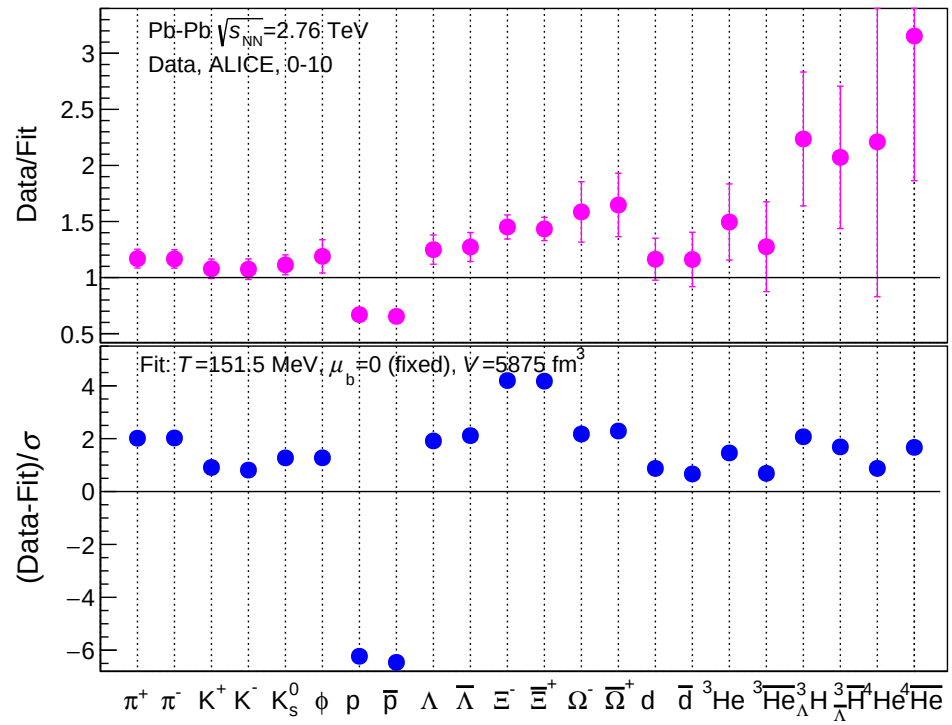

Figure 9: Relative difference between data and best fit using the modified hadron spectrum 1

4.3.3 Fit using the modified hadron spectrum 2

First, the influence of the further implementation of strange baryon resonances is studied. In figures 10 and 11 the fit and relative differences for the modified hadron spectrum 1 are shown.

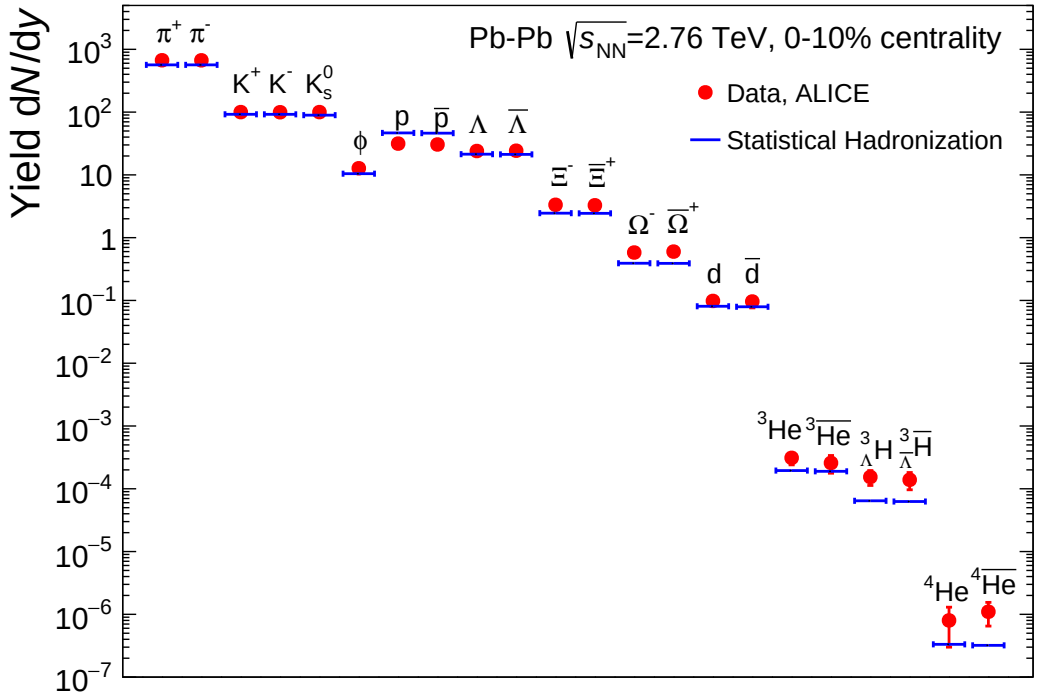

Figure 10: Particle multiplicities measured at ALICE with best fit using the modified hadron spectrum 2

As it was already expected from the p/π-ratio, the fit yields a slightly decreased freeze-out temperature of $T_{ch} = 151.0$ MeV. The fit improves a little with a reduced $\chi^2/d.o.f.$ of 144/20 and the deviations of the proton yields are decreased to 6.0σ and 6.3σ for protons and antiprotons, respectively. The improvement of the fit is mainly due to the increased yields of the strange baryons with decreased deviations for the yields of (anti-)Λ, (anti-)Ξ and (anti-)Ω by about 1σ, 0.5σ and 0.3σ, respectively.
These results show that the problem of the large deviations of the proton yields cannot be solved by implementing just additional baryon states to the hadron spectrum.

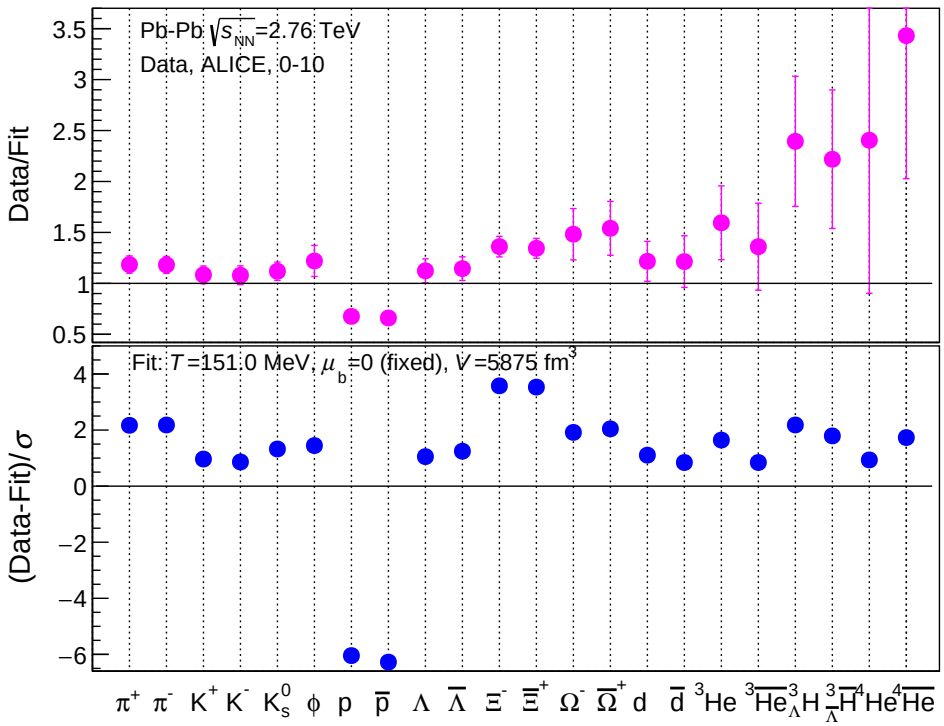

Figure 11: Relative difference between data and best fit using the modified hadron spectrum 2

4.3.4 Fit using the modified hadron spectrum 3

The influence of including meson states in addition to the baryon states - and thus restoring the balance of the included hadrons - is presented in this part.
Figures 12 and 13 show the fit and the relative differences for the modified hadron spectrum 3.

Implementing meson states has only little influence on the yields and the fit parameters. The extracted freeze-out temperature is T_{ch} = 151.5 MeV, the same as it was with included non-strange baryons. With a reduced $\chi^2/d.o.f.$ of 143/20 the quality of the fit is almost unchanged. The same applies to the deviations of the proton yields.

The results presented in the last two parts show that a restoration of the balance of implemented hadron species, does not significantly reduce the deviations of the proton yields. This means that the reason for the deterioration of the fit is not an imbalance of the hadron spectrum but it has to be explained differently.

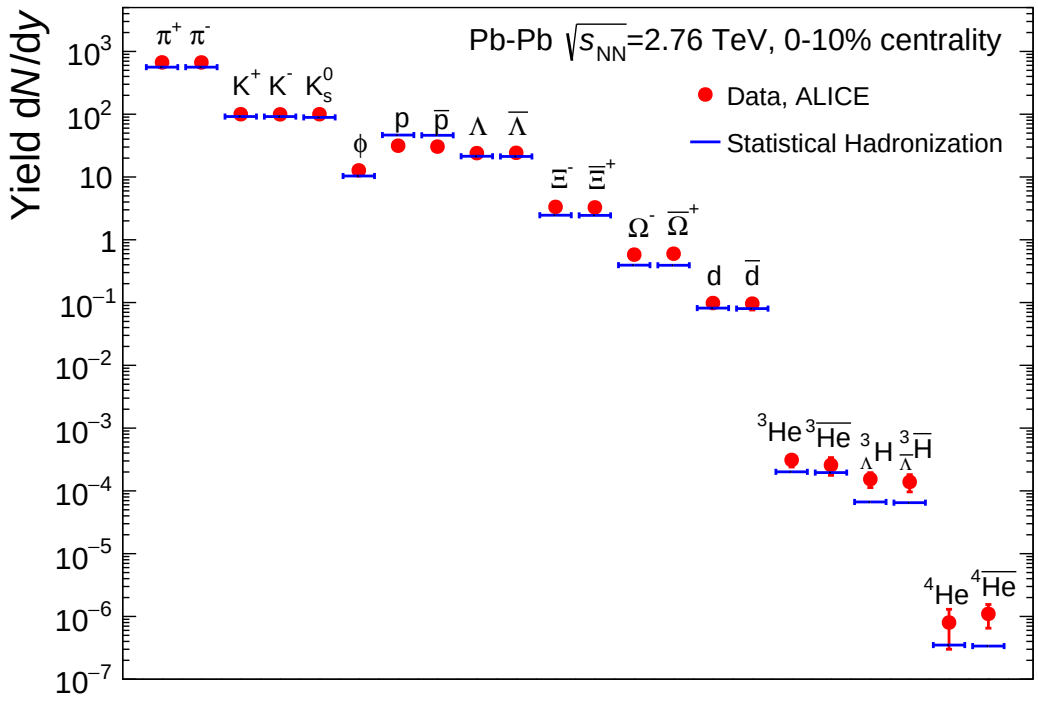

Figure 12: Particle multiplicities measured at ALICE with best fit using the modified hadron spectrum 3

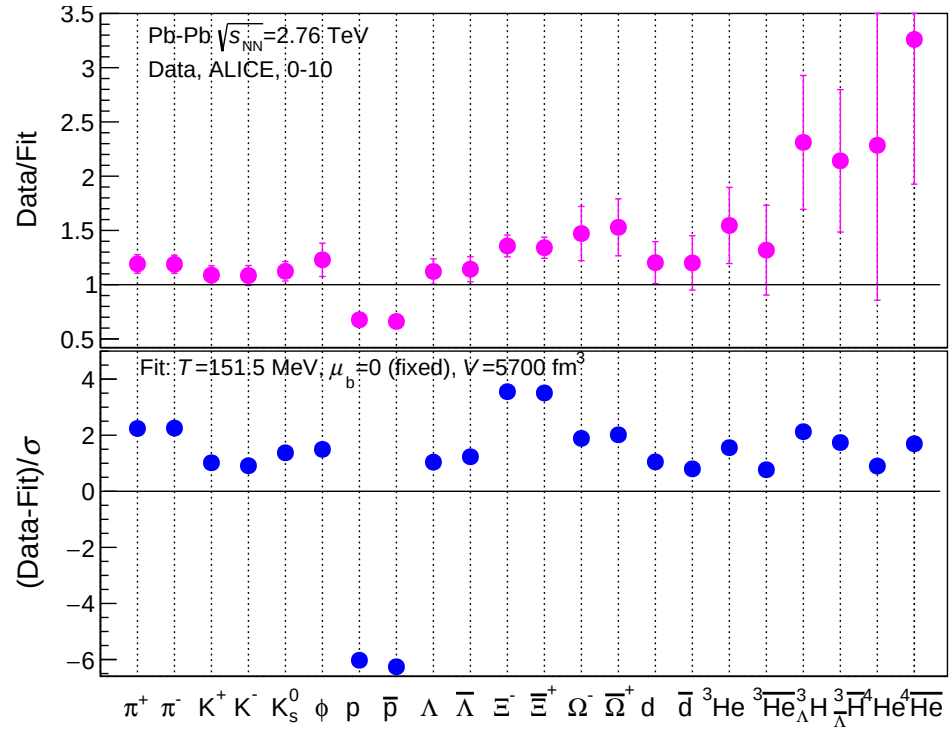

Figure 13: Relative difference between data and best fit using the modified hadron spectrum 3

4.4 Correction with the S-matrix formalism

In [26] a different approach to improve the proton anomaly was presented.
The equations as presented in section 2 describe a hadron resonance gas (HRG). In this approach, resonances are treated as an ideal gas and resonance widths are neglected.
Statistical mechanics can be formulated in terms of the S-matrix [15]. This makes it possible to explicitly consider resonant and non-resonant interactions in the description of the hadron gas produced in heavy-ion collisions.
In [26] the effect of two-body interactions in the πN system is studied. Within the S-matrix treatment, these are considered by using measured phase shifts.
This treatment results in a suppression of the proton yields as shown in figure 14.

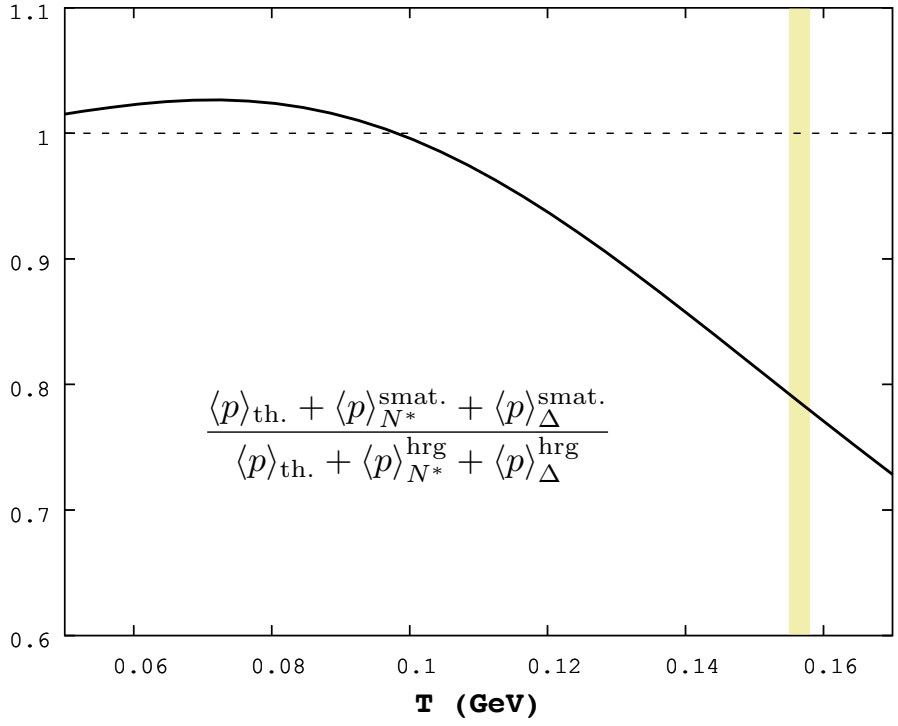

Figure 14: Ratio between proton yields calculated within the S-matrix and the HRG approach [27]

The thermal fit using the S-matrix correction leads to a reduction of the deviations for the (anti-)proton yields to less than 1σ with an extracted freeze-out temperature of $T_{ch} = 155.0$ MeV and a $\chi^2/d.o.f.$ of 19.7/19. Using this correction, the proton anomaly is no longer observable.
This correction can also be applied to the modified hadron spectrum in order to check if it is able to explain the large deviations appearing in the fits. For simplicity the ratios as presented in [26] are taken.

Figures 15 and 16 show the fit with the modified hadron spectrum 3 with applied S-matrix correction.

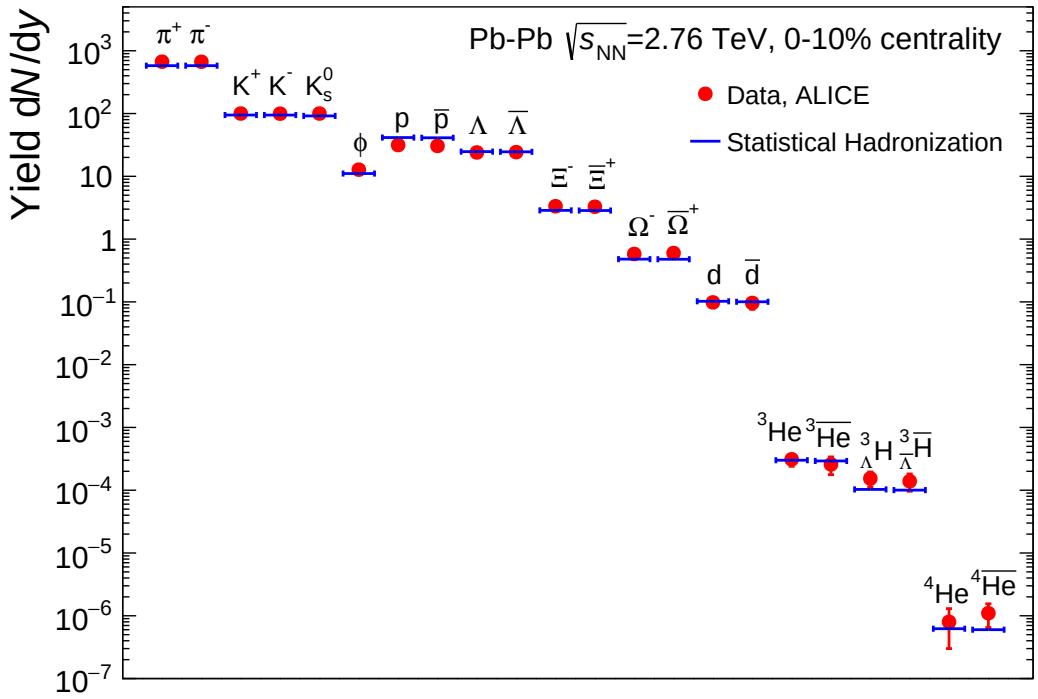

Figure 15: Particle multiplicities measured at ALICE with best fit using the modified hadron spectrum 3 with applied S-matrix correction

Applying the correction, leads to a significantly improved fit. The $\chi^2/d.o.f.$ decreases to 57.5/20 and the extracted freeze-out temperature rises to $T_{ch} = 156.0$ MeV, close to the temperature extracted from the fit using the unmodified spectrum. Nevertheless there is still a deviation of the proton yields with 4σ and 4.2σ for protons and antiprotons, respectively.

As seen from the density ratios shown in figure 5, the proton yields are affected to the highest extent by the implementation of new states.

Excluding the protons from the fit with applied S-matrix correction - as shown in figures 17 and 18 - leads to a reduced $\chi^2/d.o.f.$ of 10.7/18 and a freeze-out temperature of $T_{ch} = 156.0$ MeV. This means that the other calculated particle yields are in good agreement with the measurements. The measured proton yields are now about 30% below the calculations, corresponding to a deviation of about 6σ.

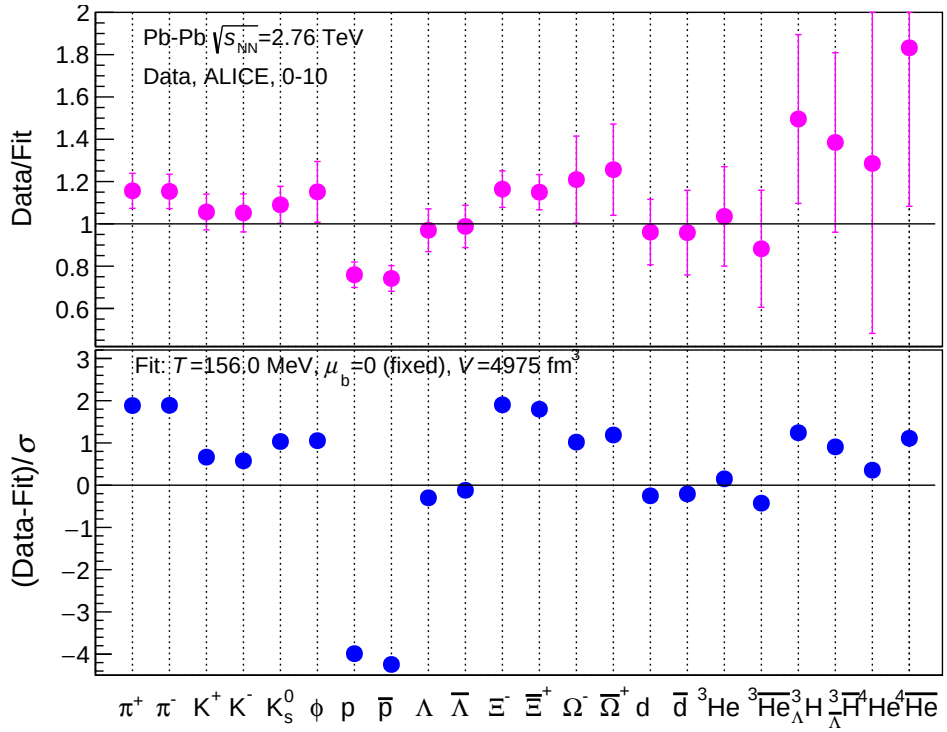

Figure 16: Relative difference between data and best fit using the modified hadron spectrum 3 with applied S-matrix correction

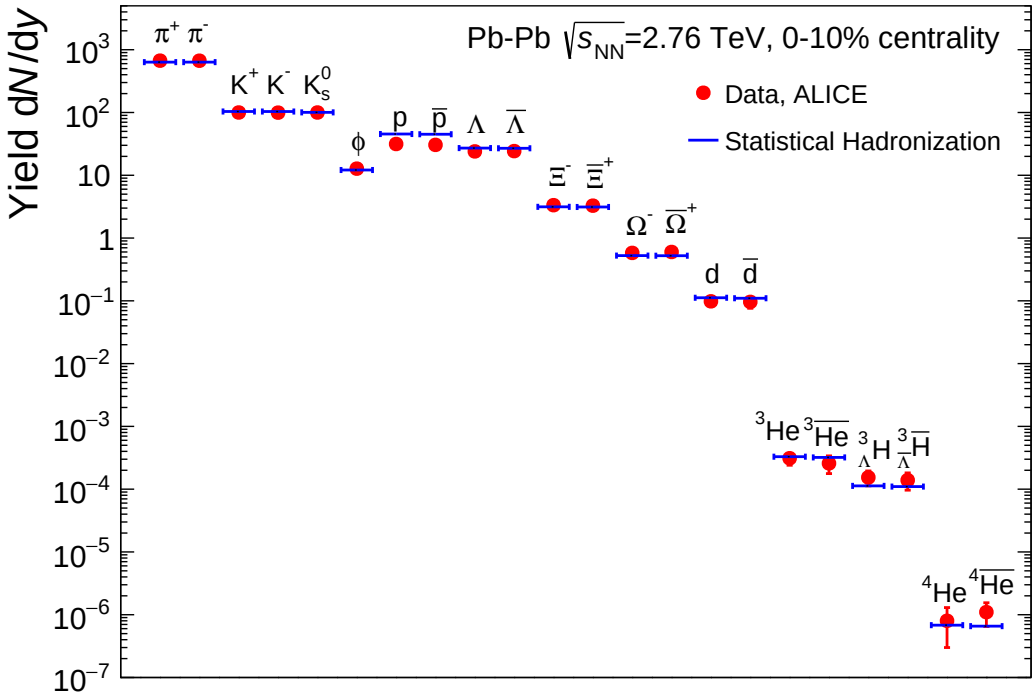

Figure 17: Particle multiplicities measured at ALICE with best fit using the modified hadron spectrum 3 and excluding the corrected proton yields

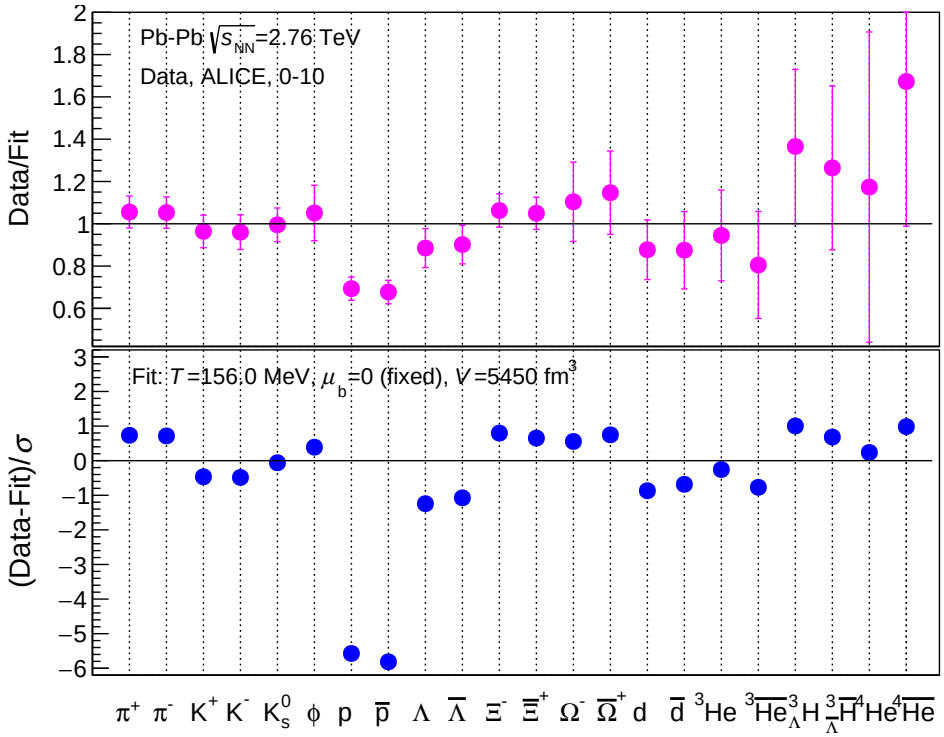

Figure 18: Relative difference between data and best fit using the modified hadron spectrum 3 and excluding the corrected proton yields

The results from the S-matrix correction and the fit with excluded protons show that the S-matrix treatment cannot solve the problem of large deviations in the case of the modified spectra.

The problem with the implementation of theoretical states into the hadron spectrum is the little information about the resonances obtained from the calculations. The only known properties are the mass, total spin and parity. This means that these states not only contain well defined discrete resonances, but also several broad resonances. These broad resonances cannot be approximated as a delta function but form a kind of continuum distribution. Therefore they cannot be counted as a separate particle.
Furthermore, the failure of the S-matrix correction shows that some of these resonances are not produced in interactions between more than two particles. These are not considered in the S-matrix approach as presented in [26]. The influence of these states is highly overestimated in the picture of a hadron resonance gas and cannot be corrected by the S-matrix approach.

5 Conclusion

In this work, the influence of the implementation of theoretical hadron states on hadron densities calculated in the framework of the statistical hadronization model was studied. The calculated densities were fitted to measurements from the ALICE experiment in order to obtain the chemical freeze-out temperature T_{ch}. The baryochemical potential was fixed to $\mu_b = 0$ MeV.

The main objective of the study was to investigate reasons for the appearing proton anomaly and the deterioration of the fit with included non-strange baryons, as seen in an earlier study.

The dependence of the p/π-ratio on the hadron spectrum and the temperature was examined. In combination with the particle ratios, this showed that including baryon states increases the ratio, leading to a decreasing freeze-out temperature, whereas additional meson states have the opposite effect.

This strengthened the idea that the imbalance in the included hadrons could be responsible for the deterioration of the fit with the included non-strange baryons.

The additional non-strange baryons in the spectrum led to an increased deviation of the proton yields of more than 6σ and a drop in the freeze-out temperature to 150.0 MeV in the original study, which could be increased to 151.5 MeV due to a changed underlying hadron spectrum. The highly overestimated proton yields lead to increasing deviations of the other particle yields and an overall deterioration of the fit with a strongly increased $\chi^2/d.o.f.$ of 161/20.

The further implementation of strange baryon resonances had a similar but weaker effect as the non-strange states. As expected from the p/π-ratio, the freeze-out temperature further decreased to 151.0 MeV and the fit improved with a slightly decreased $\chi^2/d.o.f.$ of 144/20. Nevertheless the proton yields still deviate by around 6σ from the data.

Due to the relatively high masses of the inserted mesons ($\gtrsim 1.5$ GeV), inserting additional meson states did not have a significant influence. The temperature increased again to 151.5 MeV.

These results showed that the large deviations from the included non-strange baryons cannot be compensated by completing the set of hadrons.

A correction, using a description of statistical mechanics in terms of the S-matrix, was applied to the calculations with the modified hadron spectrum.

It was shown before that this approach was able to solve the proton anomaly for the unmodified hadron spectrum. In this work it was tested, if it could also explain the deviations coming from the implemented theoretical hadron states.

Applying the correction led to a major improvement of the fit.

The $\chi^2/d.o.f.$ strongly decreased to 57.5/20 and the temperature rose to 156.0 MeV, about the same temperature obtained from the fit with the unmodified hadron spectrum. However, the deviations in proton yields were still about 4σ. Furthermore a fit with applied S-matrix correction but excluded protons showed that the calculated yields for the other

particles were in agreement with the measurements and the fit gave a temperature of 156.0 MeV.
This showed that the S-matrix approach is not able to explain the large deviations caused by the theoretical states.

The reason for the deteriorated fit is that it is not possible to simply add theoretically predicted states into the statistical hadronization model. Some of these states do not appear as discrete resonances but as a continuum. Additionally, the resonance states are not necessarily produced by two-body interactions. This makes it impossible two apply the S-matrix correction as used here.

As a result, only resonance states observed in experiments can be included in the statistical hadronization model in an, a priori, reasonable way.
Due to unknown states this leads to a systematic error in the description of heavy-ion collisions. In order to quantify this error, further studies of extended hadron spectra may be useful. However, these studies have to be carefully evaluated and interpreted, because of the unknown origin of theoretical resonance states.

A Properties of included baryons

name	**mass [MeV]**	J^P	**strangeness**
$\Lambda(1618)$	1618	$\frac{3}{2}^-$	-1
$\Lambda(1869)$	1869	$\frac{1}{2}^+$	-1
$\Lambda(1880)$	1880	$\frac{1}{2}^+$	-1
$\Lambda(1943)$	1943	$\frac{3}{2}^+$	-1
$\Lambda(1969)$	1969	$\frac{3}{2}^+$	-1
$\Lambda(2012)$	2012	$\frac{3}{2}^+$	-1
$\Lambda(2025)$	2025	$\frac{3}{2}^+$	-1
$\Lambda(2033)$	2033	$\frac{5}{2}^+$	-1
$\Lambda(2035)$	2035	$\frac{3}{2}^+$	-1
$\Lambda(2049)$	2049	$\frac{3}{2}^+$	-1
$\Lambda(2057)$	2057	$\frac{5}{2}^+$	-1
$\Lambda(2073)$	2073	$\frac{1}{2}^+$	-1
$\Lambda(2085)$	2085	$\frac{1}{2}^+$	-1
$\Lambda(2094)$	2094	$\frac{5}{2}^+$	-1
$\Lambda(2118)$	2118	$\frac{3}{2}^+$	-1
$\Lambda(2151)$	2151	$\frac{5}{2}^-$	-1
$\Lambda(2164)$	2164	$\frac{7}{2}^+$	-1
$\Lambda(2165)$	2165	$\frac{1}{2}^+$	-1
$\Lambda(2186)$	2186	$\frac{5}{2}^-$	-1
$\Lambda(2188)$	2188	$\frac{1}{2}^-$	-1
$\Lambda(2202)$	2202	$\frac{3}{2}^-$	-1
$\Lambda(2215)$	2215	$\frac{1}{2}^-$	-1
$\Lambda(2220)$	2220	$\frac{1}{2}^+$	-1
$\Lambda(2220)$	2220	$\frac{1}{2}^-$	-1
$\Lambda(2230)$	2230	$\frac{5}{2}^-$	-1
$\Lambda(2231)$	2231	$\frac{3}{2}^-$	-1
$\Lambda(2233)$	2233	$\frac{1}{2}^-$	-1
$\Lambda(2238)$	2238	$\frac{3}{2}^-$	-1
$\Lambda(2258)$	2258	$\frac{3}{2}^+$	-1
$\Lambda(2262)$	2262	$\frac{5}{2}^-$	-1
$\Lambda(2265)$	2265	$\frac{3}{2}^-$	-1
$\Lambda(2273)$	2273	$\frac{1}{2}^-$	-1

name	**mass [MeV]**	J^P	**strangeness**
$\Sigma(1568)$	1568	$\frac{1}{2}^-$	-1
$\Sigma(1617)$	1617	$\frac{1}{2}^-$	-1
$\Sigma(1715)$	1715	$\frac{3}{2}^-$	-1
$\Sigma(1975)$	1975	$\frac{3}{2}^+$	-1
$\Sigma(1984)$	1984	$\frac{1}{2}^+$	-1
$\Sigma(1987)$	1987	$\frac{1}{2}^+$	-1
$\Sigma(1999)$	1999	$\frac{1}{2}^+$	-1
$\Sigma(2040)$	2040	$\frac{3}{2}^+$	-1
$\Sigma(2049)$	2049	$\frac{1}{2}^+$	-1
$\Sigma(2081)$	2081	$\frac{1}{2}^+$	-1
$\Sigma(2082)$	2082	$\frac{3}{2}^+$	-1
$\Sigma(2084)$	2084	$\frac{3}{2}^+$	-1
$\Sigma(2084)$	2084	$\frac{5}{2}^+$	-1
$\Sigma(2087)$	2087	$\frac{3}{2}^+$	-1
$\Sigma(2109)$	2109	$\frac{3}{2}^+$	-1
$\Sigma(2146)$	2146	$\frac{5}{2}^+$	-1
$\Sigma(2149)$	2149	$\frac{3}{2}^+$	-1
$\Sigma(2151)$	2151	$\frac{1}{2}^+$	-1
$\Sigma(2169)$	2169	$\frac{3}{2}^+$	-1
$\Sigma(2169)$	2169	$\frac{5}{2}^+$	-1
$\Sigma(2181)$	2181	$\frac{5}{2}^+$	-1
$\Sigma(2211)$	2211	$\frac{1}{2}^+$	-1
$\Sigma(2211)$	2211	$\frac{3}{2}^-$	-1
$\Sigma(2221)$	2221	$\frac{5}{2}^-$	-1
$\Sigma(2242)$	2242	$\frac{7}{2}^+$	-1
$\Sigma(2242)$	2242	$\frac{1}{2}^-$	-1

name	**mass [MeV]**	J^P	**strangeness**
$\Xi(1760)$	1760	$\frac{1}{2}^-$	-2
$\Xi(1787)$	1787	$\frac{1}{2}^-$	-2
$\Xi(1893)$	1893	$\frac{1}{2}^-$	-2
$\Xi(1904)$	1904	$\frac{3}{2}^-$	-2
$\Xi(1944)$	1944	$\frac{3}{2}^-$	-2
$\Xi(2025)$	2025	$\frac{5}{2}^-$	-2
$\Xi(2157)$	2157	$\frac{1}{2}^+$	-2
$\Xi(2157)$	2157	$\frac{3}{2}^+$	-2
$\Xi(2175)$	2175	$\frac{1}{2}^+$	-2
$\Xi(2187)$	2187	$\frac{1}{2}^+$	-2
$\Xi(2189)$	2189	$\frac{5}{2}^+$	-2
$\Xi(2200)$	2200	$\frac{1}{2}^+$	-2
$\Xi(2227)$	2227	$\frac{3}{2}^+$	-2
$\Xi(2267)$	2267	$\frac{3}{2}^+$	-2
$\Xi(2268)$	2268	$\frac{1}{2}^+$	-2
$\Xi(2285)$	2285	$\frac{3}{2}^+$	-2
$\Xi(2290)$	2290	$\frac{3}{2}^+$	-2
$\Omega(1991)$	1991	$\frac{1}{2}^-$	-3
$\Omega(2081)$	2081	$\frac{3}{2}^-$	-3
$\Omega(2355)$	2355	$\frac{1}{2}^+$	-3
$\Omega(2392)$	2392	$\frac{3}{2}^+$	-3
$\Omega(2422)$	2422	$\frac{1}{2}^+$	-3
$\Omega(2462)$	2462	$\frac{5}{2}^+$	-3
$\Omega(2475)$	2475	$\frac{3}{2}^+$	-3

B Properties of included mesons

name	**mass (MeV)**	J^P	**strangeness**
$h_1(1380)$	1485	1^+	0
$\rho_2(1661)^+$	1661	2^-	0
$\rho_2(1661)^0$	1661	2^-	0
$\rho_2(1661)^-$	1661	2^-	0
$\omega_2(1661)$	1661	2^-	0
$a_0(1679)^+$	1679	0^+	0
$a_0(1679)^0$	1679	0^+	0
$a_0(1679)^-$	1679	0^+	0
$K(1538)^+$	1538	0^-	1
$K(1538)^-$	1538	0^-	-1
$K(1538)^0$	1538	0^-	1
$\bar{K}(1538)^0$	1538	0^-	-1
$K^*(1675)^+$	1675	1^-	1
$K^*(1675)^-$	1675	1^-	-1
$K^*(1675)^0$	1675	1^-	1
$\bar{K}^*(1675)^0$	1675	1^-	-1
$K_1(1757)^+$	1757	1^+	1
$K_1(1757)^-$	1757	1^+	-1
$K_1(1757)^0$	1757	1^+	1
$\bar{K}_1(1757)^0$	1757	1^+	-1
$K_0^*(1791)^+$	1791	0^+	1
$K_0^*(1791)^-$	1791	0^+	-1
$K_0^*(1791)^0$	1791	0^+	1
$\bar{K}_0^*(1791)^0$	1791	0^+	-1

References

[1] G. Aad et al. Observation of a new particle in the search for the Standard Model Higgs boson with the ATLAS detector at the LHC. *Phyics Letters*, B716:1-29, 2012

[2] S. Chatrchyan et al. Observation of a new boson at a mass of 125 GeV with the CMS experiment at the LHC. *Physics Letters*, B716:30-61, 2012

[3] P. W. Higgs. Broken symmetries and the masses of gauge bosons. *Physical Review Letters*, 13:508-509, 1964

[4] F. Englert and R. Brout. Broken Symmetry and the Mass of Gauge Vector Mesons. *Physical Review Letters*, 13:321-323, 1964

[5] R. Alkofer and J. Greensite. Quark confinement: the hard problem of hadron physics. *Journal of Physics G: Nuclear and Particle Physics*, 34:S3, 2007

[6] F. Wilczek. Asymptotic freedom: From paradox to paradigm. *PNAS*, 102:8403-8413, 2005

[7] P. Foka , M. A. Janik. An overview of experimental results from ultra-relativistic heavy-ion collisions at the CERN LHC: Bulk properties and dynamical evolution. *Review in Physics*, 1:154-171, 2016

[8] Roy A. Lacey, N. N. Ajitanand, J. M. Alexander, P. Chung, W. G. Holzmann, M. Issah, A. Taranenko, P. Danielewicz, and Horst Stöcker. Has the QCD Critical Point Been Signaled by Observations at the BNL Relativistic Heavy Ion Collider? *Physical Review Letters*, 98:092301, 2007

[9] Mikhail Stephanov. QCD phase diagram and the critical point. *Progress of Theoretical Physics Supplement*, 153:139-156, 2004

[10] H.-T. Ding, F. Karsch, S. Mukherjee. Thermodynamics of Strong-Interaction Matter from Lattice QCD. *Quark-Gluon Plasma*, 5:1-66, 2016

[11] I. Arsene et al. Quark-gluon plasma and color glass condensate at RHIC? The perspective from the BRAHMS experiment. *Nuclear Physics*, A757:1-27, 2005

[12] P. Braun-Munzinger, J. Stachel, C. Wetterich. Chemical freeze-out and the QCD phase transition temperature. *Physics Letters*, B596:61-69, 2004

[13] C. Blume. Is there Life after Hadronization? An Experimental Overview. *Acta Physica Polonica*, B43:577-584, 2012

[14] F. Schwabl. *Statistische Mechanik*. Springer-Verlag, 3. aktualisierte Auflage, 2006

[15] R. Dashen, S.-k. Ma and H.J. Bernstein. S-Matrix Formulation of Statistical Mechanics. *Physical Review*, 187:345-370, 1969

[16] D. H. Rischke, M. I. Gorenstein, H. Stöcker, W. Greiner. Excluded volume effect for the nuclear matter equation of state. *Zeitschrift für Physik C - Particles and Fields*, 51:485-489, 1990

[17] P. Braun-Munzinger, J. Stachel, J.P. Wessels, N. Xu. Thermal and hadrochemical equilibration in nucleus-nucleus collisions at the SPS. *Physics Letters*, B365:1-6, 1996

[18] P. Braun-Munzinger, D. Magestro, K. Redlich, J. Stachel. Hadron production in Au-Au collisions at RHIC. *Physics Letters*, B518:41-46, 2001

[19] J. Stachel et al. Confronting LHC data with the statistical hadronization model. *Journal of Physics: Conference Series*, 509:012019, 2014

[20] A. Andronic, P. Braun-Munzinger, K. Redlich and J. Stachel. The statistical model in Pb-Pb collisions at the LHC. *Nuclear Physics*, A904-905:535c-538c, 2013

[21] D. Gündüz. Study of the influence of modified light flavour hadron spectra on thermal model hadron densities. Bachelor Thesis, Heidelberg, 2015

[22] R. G. Edwards, N. Mathur, D. G. Richards and S. J. Wallace. Flavor structure of the excited baryon spectra from lattice QCD. *Physical Review*, D87:054506, 2013.

[23] D. Ebert, R. N. Faustov, and V. O. Galkin. Mass spectra and Regge trajectories of light mesons in the relativistic quark model. *Physical Review*, D79:114029, 2009

[24] M. Tanabashi et al. (Particle Data Group). Review of Particle Physics. *Physical Review*, D98:030001, 2018

[25] A. Andronic, P. Braun-Munzinger, K. Redlich and J. Stachel. Hadron yields, the chemical freeze-out and the QCD phase diagram. *Journal of Physics: Conference Series*, 779:012012, 2017

[26] A. Andronic, P. Braun-Munzinger, B. Friman, P. M. Lo, K. Redlich and J. Stachel. The thermal proton yield anomaly in Pb-Pb collisions at the LHC and its resolution. arXiv:hep-ph/1808.03102

[27] P. M. Lo, B. Friman, K. Redlich, C. Sasaki. S-matrix analysis of the baryon electric charge correlation. *Physics Letters*, B778:454-458, 2018

Acknowledgement

At first, I would like to thank Prof. Dr. Johanna Stachel for giving me the oppoertunity to work in the ALICE group and to study such an interesting topic.

I would like to especially thank Markus Köhler, who helped me a lot with appearing problems and questions and comments to my thesis. Without this support, this bachelor thesis wouldn't have been possible.

Furthermore I would like to thank everyone else involved in this thesis, especially Dr. Anton Andronic for providing the code for the calculations.

At last, I want to thank my family and friends for all the support and distraction from work in the last years.

Erklärung

Ich versichere, dass ich diese Arbeit selbstständig verfasst und keine anderen als die angegebenen Quellen und Hilfsmittel benutzt habe.

Heidelberg, den 03.09.2018,